JOURNAL OF CATALYSIS 96, 88–105 (1985)

Studies of the Interactions of H_2 and CO with Silica- and Lanthana-Supported Palladium[1]

JEFFERY S. RIECK AND ALEXIS T. BELL

Materials and Molecular Research Division, Lawrence Berkeley Laboratory and Department of Chemical Engineering, University of California, Berkeley, California 94720

Received November 29, 1984; revised June 3, 1985

The interactions of H_2 and CO with Pd/SiO_2, Pd/La_2O_3, and lanthana-promoted Pd/SiO_2 have been investigated using temperature-programmed desorption and temperature-programmed surface reaction. These studies reveal that in the presence of lanthana, a portion of the lanthana in close contact with the Pd particles undergoes reduction to form LaO_x moieties. These species cause a reduction in the absolute magnitude of H_2 and CO adsorption, as well as a change in the distribution of adstates. The latter effect is relatively small for H_2 but is quite significant for CO, for which it is found that adsorption into strongly bound states is suppressed more extensively than adsorption into weakly bound states. The LaO_x moieties also facilitate the dissociation of CO, a key step in CO methanation and, as a consequence, the synthesis of CH_4 over Pd/La_2O_3 and lanthana-promoted Pd/SiO_2 is much more rapid than that over Pd/SiO_2. The change in the distribution of adsorbed H_2 and CO under synthesis conditions, brought about by LaO_x, also contributes to the higher selectivity of the lanthana-containing catalysts for methanol synthesis.

INTRODUCTION

Depending on the composition of the support used, high selectivities of methanol or methane can be achieved during CO hydrogenation over dispersed palladium (*1–16*). Lanthana is a particularly attractive support because it permits the achievement of combined high selectivity and specific activity for methanol synthesis. In a recent series of studies, Hicks *et al.* (*15–18*) described the physical and catalytic properties of lanthana-supported Pd catalysts and compared these with the properties of silica-supported Pd. The results of XPS, IR spectroscopy, and chemisorption experiments indicated that Pd supported on silica shows no evidence for a metal–support interaction. The opposite was found for lanthana-supported Pd. XPS spectroscopy revealed evidence for a change in the electronic properties of Pd. This was attributed to the presence of patches of partially reduced LaO_x residing on the surface of the metal particles. This picture was further supported by the observation that as the coverage of the Pd particles by LaO_x increases, the CO chemisorption capacity of the catalyst decreases.

The present studies were undertaken to further investigate the ideas proposed by Hicks *et al.* (*17, 18*). In particular, experiments were carried out to characterize the strengths of H_2 and CO adsorption on Pd/La_2O_3, Pd/SiO_2, and lanthana-promoted Pd/SiO_2. The influence of support composition on the dissociation of CO and on CO hydrogenation were also investigated. The extent to which lanthana can be reduced by H_2 was studied as well. Temperature-programmed reduction (TPR), temperature-programmed desorption (TPD), and temperature-programmed surface reaction (TPSR) were used as the principal methods for probing the interactions of H_2 and CO with the catalysts.

EXPERIMENTAL

Apparatus

The apparatus used for the present study has been described previously (*19–21*). The

[1] The U.S. Government's right to retain a nonexclusive royalty-free license in and to the copyright covering this paper, for governmental purposes, is acknowledged.

0021-9517/85 $3.00

TABLE 1

Catalyst Properties

Catalyst	Dispersion[a] (%)	Saturation coverage[b]		Mass (mg)
		H_2	CO	
9% Pd/SiO_2	18	—	1.10	25
2% Pd/SiO_2	35	1.05	1.10	58
8.8% Pd/La_2O_3	8	—	0.0	58
1.9% Pd/La_2O_3	16	0.83	0.34	134
4.8% La/(2% Pd/SiO_2)	35	—	—	58

[a] Based on H_2–O_2 titration.
[b] Reported as the ratio of the moles of H or CO adsorbed per surface Pd atom determined by H_2–O_2 titration.

catalysts were contained in a quartz microreactor which could be heated at up to 1 K/s. The desorbing gas was swept from the microreactor by a continuous flow of carrier gas. Analysis of the effluent flow was performed with a quadrupole mass spectrometer. The transfer time from the microreactor to the mass spectrometer was less than 1.5 s. A microprocessor-based data acquisition system was used to direct the mass spectrometer to a series of preselected masses and to record the signal intensity at each mass setting. The catalyst temperature was also recorded by the data acquisition system.

Materials

The preparation and characterization of the Pd/SiO_2 and Pd/La_2O_3 catalysts have been described previously (*17, 18*). The Pd/SiO_2 catalysts were obtained by incipient wetness impregnation of Cab-O-Sil HS-5 silica with a solution of H_2PdCl_4 dissolved in 1 *N* HCl. The Pd/La_2O_3 catalysts were prepared through ion exchange of H_2PdCl_4 and $La(OH)_3$. The samples were dried, calcined in a 21% O_2/He mixture at 623 K for 2 h, and reduced in H_2 and 573 K for 3 h. These catalysts were then characterized by H_2–O_2 titration and H_2 and CO chemisorption. The results of the characterization experiments are listed in Table 1.

The procedure for the preparation of the lanthana-promoted Pd/SiO_2 catalyst was somewhat different. A portion of the 2% Pd/SiO_2 catalyst was removed after the calcination step. The calcined catalyst was impregnated with a solution of $La(NO_3)_3$ in deionized water and dried. The catalyst was calcined again to decompose the $La(NO_3)_3$ and reduced in H_2 at 573 K for 3 h. This catalyst was also characterized using H_2–O_2 titration.

Helium (99.998%) was purified of O_2 to less than 200 ppb by passage through an Oxyclear (Labclear) filter. High-purity H_2 (99.999%) was passed through a Deoxo purifier (Engelhard) to convert O_2 impurities to water. The H_2 and He were then passed through liquid-N_2-cooled traps filled with Linde 13X molecular sieve to remove water. Ultrahigh purity CO (99.99%) was passed through a bed of glass beads heated to 623 K to decompose metal carbonyls, a dry-ice-cooled trap filled with Linde 13X molecular sieve to remove water, and finally through an Ascarite filled trap to remove CO_2. In addition to the pure gases, mixtures of 1000 ppm H_2 and 408 ppm CO in ultrapure He were available for adsorption. The 1000 ppm H_2 in ultrapure He also served as the reducing mixture in the temperature-programmed reduction experiments, and a mixture of 1000 ppm O_2 in He was available for temperature-programmed oxidation experiments. The mass spectrometer was used to verify that no impurities were present in any of the gases.

Experimental Procedure

Temperature-programmed desorption. The procedure for all TPD experiments was similar. The catalysts were sieved to obtain 30/60 mesh granules. Calculations by Rieck and Bell (*22*) have shown that the intraparticle mass transfer resistance for particles of this size is negligible. A mass of catalyst corresponding to 3.8×10^{-6} mol of surface palladium atoms based on H_2–O_2 titration was placed in the microreactor. In all cases, this resulted in a bed thickness of less than 2 mm. The mass of each catalyst used is given in Table 1. The air in the microreactor

was evacuated with a mechanical pump, and the reactor was backfilled with He. The catalysts were reduced for 4 h in 200 cm^3/min of H_2 at 573 K. Following reduction, the microreactor was evacuated and heated to 873 K at 0.25 K/s. The catalyst was cooled to room temperature while still under vacuum. At this point, the reactor was repressurized with He.

Adsorption was carried out in several ways. To saturate the catalysts, pulses of the pure gas were passed through the catalyst bed. To achieve partial coverages, a mixture of the adsorbate in He was passed through the bed for the desired amount of time or delivered in pulses. Although the adsorption methods used to achieve partial coverages may result in intraparticle gradients in coverage, modeling studies have shown this to have no effect on the spectra (*22*). After the adsorption of H_2, the catalyst was evacuated for 30 min to ensure complete removal of the hydride. For CO adsorption, the catalyst was evacuated for 10 min to remove the adsorbate remaining in the gas phase. The reactor was then repressurized with He and the He flow rate set to 50 cm^3/min. Heating of the catalyst was now commenced at 1 K/s, and the data acquisition system was activated, to initiate analysis of the desorbing gas. The experiments were halted when the temperature reached 873 K, to avoid sintering the catalyst. Following each experiment, the mass spectrometer was calibrated against He mixtures containing specified concentrations of H_2 and CO.

Temperature-programmed surface reaction. For the TPSR experiments, the catalysts were reduced as for a TPD experiment. The microreactor was then evacuated and heated to 673 K at 0.25 K/s. The catalyst was held at 673 K for 5 min, cooled to room temperature, and pressurized with He. A flow of 100 cm^3/min of the desired adsorption mixture—either pure CO or a H_2/CO mixture—was passed through the microreactor. The microreactor was ramped at 1 K/s to the desired adsorption temperature and held at that temperature for 10 min. The catalyst was then evacuated at that temperature for 5 min, cooled to room temperature, and evacuated for 10 min. Next, the catalyst was pressurized with He, and a flow of 50 cm^3/min of H_2 was passed through the catalyst bed as the temperature was ramped at 1 K/s up to 773 K.

The relative activities of the catalysts for CO hydrogenation were determined in the following manner. The catalysts were reduced as described above, evacuated for 15 min at 573 K, and cooled to room temperature. A flow of 75 cm^3/min of H_2 and 25 cm^3/min of CO were passed through the catalyst bed and the temperature ramped at 1 K/s to 673 K. The temperature at which the methanation rate began to increase rapidly served as a basis for comparison of the catalyst activities.

Temperature-programmed reduction and oxidation. TPR experiments were conducted to determine the reducibility of the supports. At the beginning of these experiments, the catalyst was calcined at 623 K for 2 h in a 21% O_2/He mixture flowing at 200 cm^3/min, and then cooled to room temperature in the O_2/He mixture. The microreactor was evacuated to remove gas-phase O_2, and a flow of 1000 ppm H_2 in He was passed through the bed. The temperature was ramped at 0.25 K/s and the hydrogen consumption monitored.

TPO experiments were conducted in the following manner. The catalyst was reduced at 573 K for 4 h in pure H_2 flowing at 200 cm^3/min and cooled to room temperature in H_2. The microreactor was evacuated to remove the hydride and gas-phase H_2, and a flow of 200 cm^3/min of 1000 ppm O_2 in He was passed through the bed. The O_2 consumption was monitored as the catalyst temperature was ramped at 0.25 K/s.

Calibration and data analysis. The absolute rate of desorption in all experiments was determined in the following manner. To correct for mass spectrometer baseline drift, the observed intensity for each mass

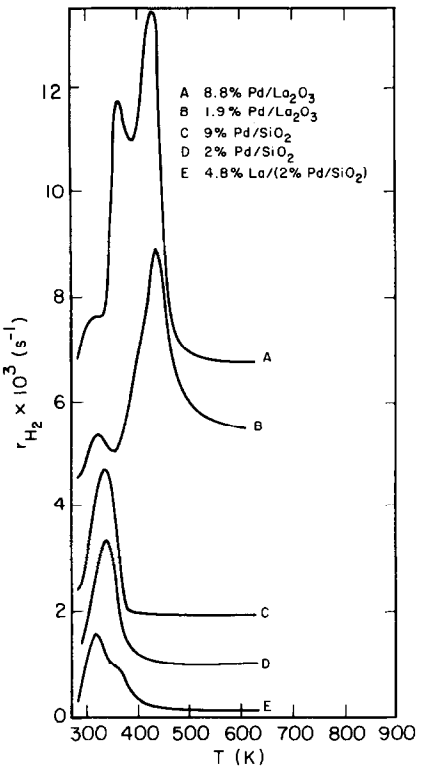

FIG. 1. H_2 consumption during TPR of calcined Pd/SiO_2, Pd/La_2O_3, and lanthana-promoted Pd/SiO_2.

was normalized with respect to the intensity of the carrier, either He or H_2. The absolute rate of desorption of species i per Pd surface site, r_i, was then determined from

$$r_i = \frac{(I_i^{obs} - I_i^{bg})}{S_i N_T} \frac{Q}{273R}, \quad (1)$$

where I_i^{obs} and I_i^{bg} are the normalized intensities for the experiment and background, respectively; S_i is the calibration factor for species i; N_T is the total number of surface Pd sites on the sample; Q is the flow rate of the carrier at STP; and R is the gas constant.

The moles of gas desorbing during an experiment were calculated by integration of the spectra to find the peak areas, A_i. The number of moles was calculated from

$$N_i = \frac{A_i}{S_i \beta} \frac{Q}{273R}, \quad (2)$$

where β is the heating rate. The initial coverages were found by dividing the number of moles desorbed by the moles of surface Pd present based on H_2–O_2 titration.

RESULTS

Temperature-Programmed Reduction and Oxidation

The spectra for H_2 consumption during the TPR experiments are shown in Fig. 1 for the five catalysts studied. The spectrum for 8.8% Pd/La_2O_3 exhibits a small shoulder at 325 K and large peaks at 367 and 433 K. The spectrum for 1.9% Pd/La_2O_3 has peaks at 328 and 440 K, but there is no peak corresponding to that seen at 367 K on the 8.8% Pd/La_2O_3. The spectra for 2% Pd/SiO_2 and 9% Pd/SiO_2 are essentially identical: both have peaks at 343 K. The lanthana-promoted Pd/SiO_2 has a peak at 323 K and a shoulder at 368 K. The integrated H_2 consumptions are given in Table 2. Also shown in this table is the amount of H_2 consumed at 298 K when H_2 is first contacted with the catalyst. An H_2 uptake at 298 K was only observed for the lanthana-containing catalysts. It is also noted that the total H_2 consumption for the Pd/La_2O_3 catalysts is significantly greater than for the Pd/SiO_2 catalysts. No uptake of H_2 was observed when La_2O_3 was subjected to TPR.

The TPO experiments revealed that, aside from an uptake at room temperature, the Pd/SiO_2 catalysts have only a slight consumption of O_2. The La_2O_3-supported catalysts, however, consumed a large amount of O_2 at elevated temperatures. The peak temperature for O_2 consumption for

TABLE 2

H_2 Consumption during TPR

Catalyst	H_2 consumption at 298 K (mol)	H_2 consumption during TPR (mol)
2.0% Pd/SiO_2	0	1.12×10^{-5}
8.8% Pd/SiO_2	0	1.15×10^{-5}
1.9% Pd/La_2O_3	2.74×10^{-6}	3.74×10^{-5}
9.0% Pd/La_2O_3	3.22×10^{-6}	3.83×10^{-5}
4.8% La/(2.0% Pd/SiO_2)	4.20×10^{-6}	7.67×10^{-6}

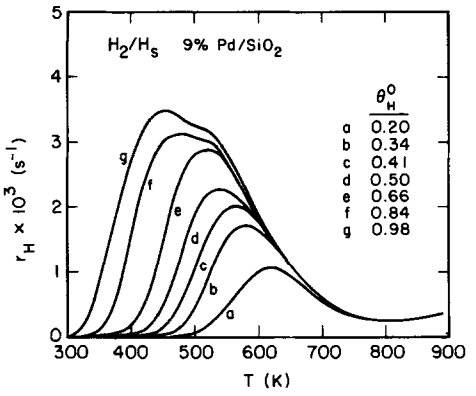

FIG. 2. Effect of initial coverage on the H_2 TPD spectra for 9% Pd/SiO_2.

1.9% Pd/La_2O_3 occurred at 561 K with a total consumption of 1.23×10^{-5} mol, while the feature for oxidation of 8.8% Pd/La_2O_3 peaked at 598 K with a consumption of 2.02×10^{-5} mol. No uptake above room temperature was observed on the 4.8% La/(2% Pd/SiO_2). The La_2O_3 support exhibited a slight uptake throughout the temperature range of the experiment.

Temperature-Programmed Desorption and Surface Reaction—Pd/SiO_2

The TPD spectra for H_2 desorption from 9% Pd/SiO_2 at varying initial coverages are shown in Fig. 2. For an initial coverage of 0.20, a single peak appears at 628 K. As the coverage is increased to 0.66, this peak shifts to 518 K, as would be expected for second-order desorption kinetics. As the coverage is increased further, a second peak appears which is centered at 458 K at full coverage. This peak also displays second-order desorption kinetics. The spectra for 2% Pd/SiO_2 are essentially the same as those for 9% Pd/SiO_2. For both catalysts, the saturation coverages were close to 1.0 indicating good agreement between the TPD experiments and H_2–O_2 titration.

The CO desoroption spectra for 2% Pd/SiO_2 are shown in Fig. 3. In addition to CO, a small amount of CO_2 desorbs at high temperatures, but no H_2 or H_2O were observed in the desorbing gas. This indicates that the water-gas shift reaction does not occur and that the formation of CO_2 results from the disproportionation of CO. The value of θ_{CO}^0 listed in Fig. 3 is the initial coverage of CO and is equal to the amount of CO desorbed, θ_{CO}, plus twice the amount of CO_2 produced. The equivalent coverage of CO converted to CO_2 is given by θ_{CO_2}. The value of θ_{CO_2} is calculated by dividing two times the moles of CO_2 produced by the number of surface Pd sites.

At $\theta_{CO}^0 = 0.21$, a single CO peak is evident at 773 K. As the initial CO coverage is increased to saturation, another peak appears at 638 K, and two low-temperature peaks appear at approximately 400 and 488 K. The CO_2 feature at saturation is shown in Fig. 11 and consists of a broad feature with a peak at 743 K. The value of θ_{CO_2} remains constant at 0.14 down to a total CO coverage of 0.57. The amount of CO_2 formed then begins to decrease, and the peak temperature increases slightly.

The TPD spectra for CO desorption from 9% Pd/SiO_2 are qualitatively quite similar to those for 2% Pd/SiO_2. The features for CO and CO_2 desorption at full coverage are shown in Fig. 4. A prominent CO peak at 668 K is accompanied by a high-temperature shoulder at about 783 K. A single low-temperature peak is seen at about 473 K; there appears to be no peak corresponding to that seen at 400 K on 2% Pd/SiO_2. The CO_2 feature is narrower than that for 2%

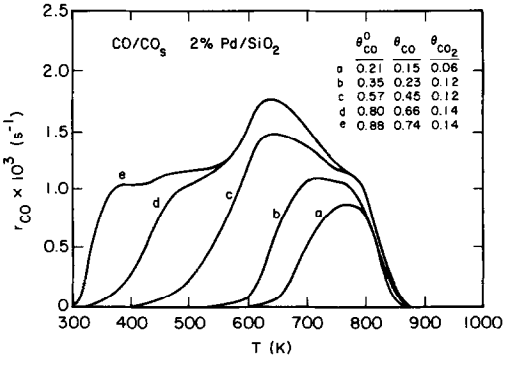

FIG. 3. Effect of initial coverage on CO desorption during CO TPD from 2% Pd/SiO_2.

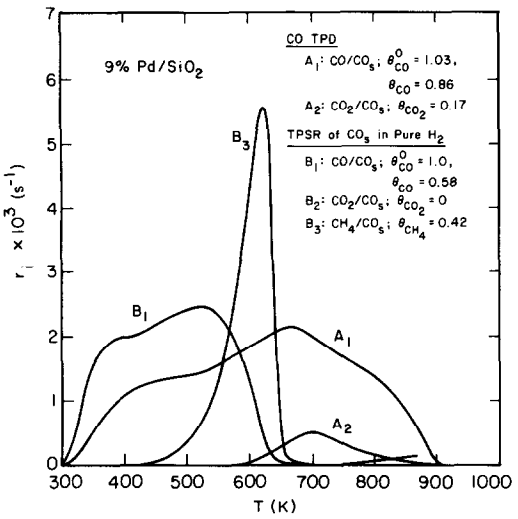

FIG. 4. Comparison of the desorption products for the TPD and TPSR of CO adsorbed on 9% Pd/SiO_2.

Pd/SiO_2 and the peak location is at 698 K. Despite these differences, though, the fraction of CO that dissociates is roughly the same for both catalysts, 7 to 8.5% The saturation coverage of CO was 1.03 for 9% Pd/SiO_2 and 0.88 for 2% Pd/SiO_2 in good agreement with earlier measurements reported by Hicks *et al.* (*18*).

A series of studies were performed in which H_2 and CO were adsorbed sequentially on the catalyst and the desorption products monitored as the temperature was ramped in a helium carrier. It was found that CO will completely displace a preadsorbed layer of H_2 while H_2 will not adsorb on a CO saturated surface. Experiments were conducted in which a partial monolayer of CO was adsorbed on the Pd/SiO_2 and the catalyst then saturated with H_2. These experiments yielded no evidence for interactions between CO and H_2 on the surface. The CO and CO_2 features were identical to those seen for the same partial coverage of CO adsorbed alone. For the same initial coverage, H_2 desorbed at lower temperatures than those observed for H_2 desorption in the absence of coadsorbed CO. This is due to the blockage by adsorbed CO of the sites for H_2 readsorption.

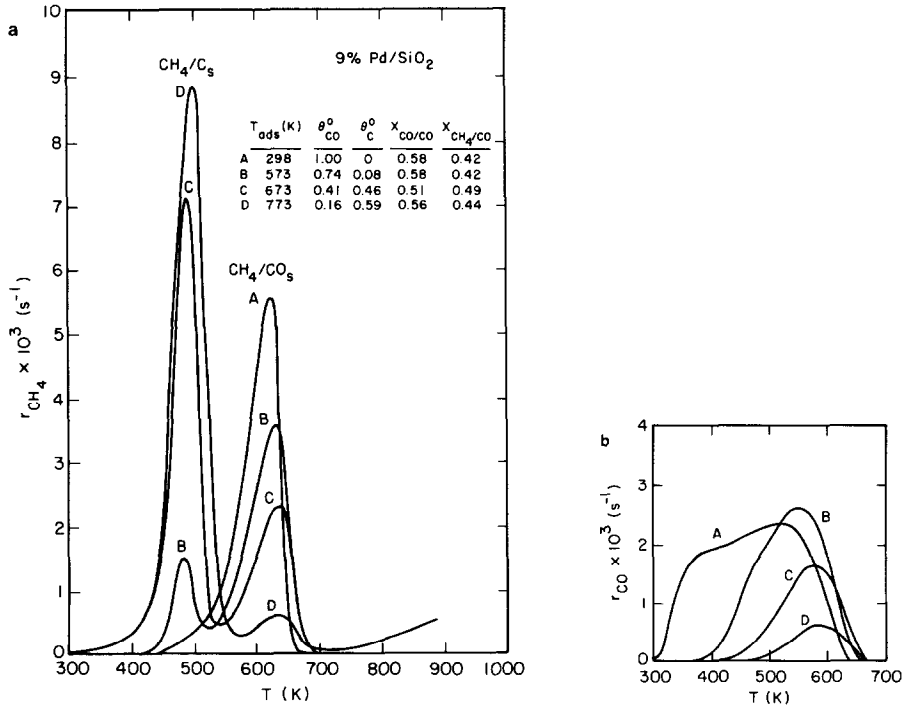

FIG. 5. Effects of CO adsorption temperature on the products formed during TPSR of CO adsorbed on 9% Pd/SiO_2: (a) CH_4; (b) CO.

In order to understand how CO and H_2 might interact on the surface of Pd, TPSR experiments were performed. The catalyst was first saturated with CO at a given temperature, cooled to room temperature under vacuum, and then heated at 1 K/s in flowing H_2. Figure 4 shows the spectra obtained for room-temperature adsorption of CO on 9% Pd/SiO_2. Also shown are the TPD spectra of the products observed for CO adsorbed to saturation level at room temperature. The TPSR spectrum shows a large CH_4 peak centered at 635 K and two overlapping CO peaks. θ_{CH_4} represents the monolayer equivalents of CH_4 formed. The rate of CO desorption into H_2 at low temperatures is greater than for a standard TPD experiment since the H_2 competes for adsorption sites, and hence suppresses CO readsorption. The rate of methane formation drops off sharply after the maximum, due to the depletion of CO from the surface. Note that the CH_4 production begins 110 K before the production of CO_2 during a CO TPD experiment. However, no CO_2 was observed during the TPSR experiments. Results similar to those shown in Fig. 4 were also obtained using the 2% Pd/SiO_2 catalyst.

Figure 5a illustrates the influence of the CO adsorption temperature on the CH_4 features observed during the TPSR experiments carried out on the 9% Pd/SiO_2 sample. The spectra for CO desorption during the ramp in H_2 are given in Fig. 5b. For adsorption temperatures above 573 K, a new methane peak appears at around 488 to 498 K. This peak is attributed to the hydrogenation of surface carbon formed during the high-temperature adsorption step. As the temperature of adsorption is increased, the methane peak resulting from the hydrogenation of adsorbed carbon increases, while that resulting from adsorbed CO decreases. The amount of CO desorbing without reaction also decreases with increasing adsorption temperature. The table contained in Fig. 5a lists θ^0_{CO}, the initial coverage of the surface by CO; θ^0_C, the initial coverage of the surface by carbon; $X_{CO/CO}$, the fraction of adsorbed CO which desorbs without reacting; and $X_{CH_4/CO}$, the fraction of adsorbed CO which reacts to form CH_4. The amount of surface carbon deposited on the surface increases steadily up to $\theta^0_C = 0.59$ for an adsorption temperature of 773 K. For higher adsorption temperatures, an unreactive surface carbon is formed which cannot be hydrogenated at temperatures lower than 723 K. The amount of surface carbon formed did not change as the time for adsorption was varied from 5 to 15 min.

The deposition of carbon on the catalyst during the high-temperature adsorption of CO was confirmed in the following way. CO was adsorbed on 9% Pd/SiO_2 at 773 K, after which the temperature was reduced to 298 K. A TPD spectrum was then recorded in flowing He. Only 0.15 monolayers of CO desorbed in this case, even though the total amount of carbon-containing species on the catalyst was 0.75 monolayers, as determined by TPSR (see Fig. 5).

Since it is uncertain what role H_2 may play in the dissociation of CO, the TPSR experiments were repeated using a mixture of 10% H_2 in CO as the adsorbate. Figure 6a shows the CH_4 features for an adsorption temperature of 573 K, and Fig. 6b shows the CO features. Note that the presence of H_2 in the adsorption mixture results in a fourfold increase in the magnitude of the peak at 488 K. However, the magnitude of the second peak decreases only slightly. In addition, the amount of unreacted CO which desorbs decreases. Thus, it appears that the presence of H_2 promotes the buildup of surface carbon. The influence of varying the H_2/CO ratio as well as the adsorption temperature on this effect is summarized in Table 3. Notice that even at an adsorption temperature of 473 K, the presence of H_2 has a significant effect on the dissociation of CO.

Pd/La_2O_3 and La-Promoted Pd/SiO_2

The H_2 desorption spectra for varying initial coverages on 1.9% Pd/La_2O_3 are

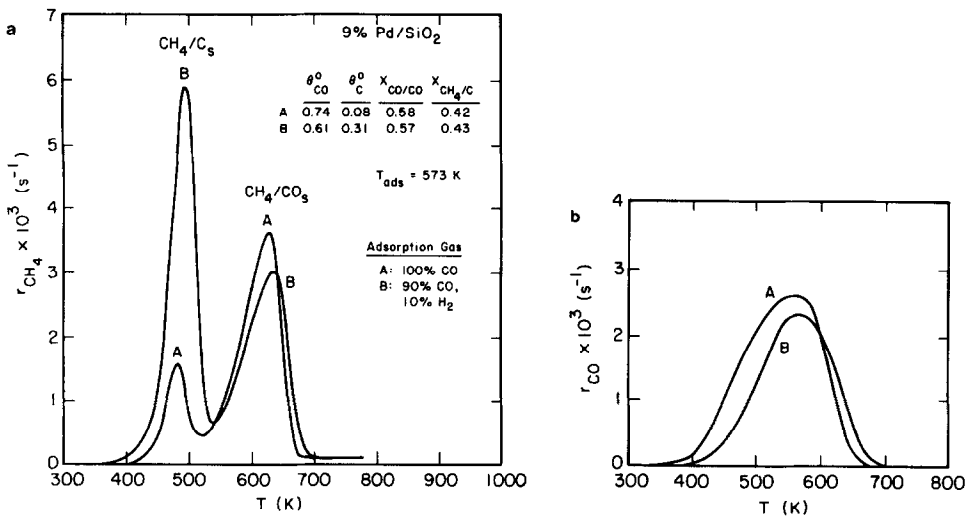

FIG. 6. Effects of the presence of H_2 during CO adsorption on the products formed during TPSR for 9% Pd/SiO_2: (a) CH_4; (b) CO.

given in Fig. 7. Notice that at 873 K a significant amount of desorption is still occurring. However, it was found that when a sample upon which no H_2 had been adsorbed was ramped to 923 K in He, no H_2 was seen to desorb until temperatures higher than 873 K were reached. Therefore, the coverages shown are based on all the H_2 desorbed up to 873 K. For an initial coverage of 0.14, no obvious peaks are present, and the H_2 desorbs only in a high-temperature tail. As the coverage is increased to 0.24, a peak becomes discernable at 698 K. This peak does not change in location or magnitude at higher coverages. A second peak appears at 593 K as the coverage is increased to 0.36. At saturation coverage, the location of this peak shifts to 533 K and a third peak appears at 423 K. Notice that the saturation coverage is 0.60, as compared to 0.83 found by H_2 chemisorption.

The H_2 desorption spectra for 8.8% Pd/La_2O_3 are very similar to those for the 1.9% Pd/La_2O_3. At saturation, the peak maxima occur at 403, 523, and 708 K, and the magnitude of the peak at 403 K relative to that at 523 K is larger than for the 1.9% Pd/

TABLE 3

Effects of H_2 on CO Dissociation over 9% Pd/SiO_2

T_{ads} (K)	Ads. mixture	θ^0_{CO}[a]	θ^0_C[b]	$X_{CO/CO}$[c]	$X_{CH_4/CO}$[d]
473	100% CO	0.81	0.02	0.62	0.38
473	90% CO, 10% H_2	0.87	0.06	0.66	0.34
523	100% CO	0.76	0.05	0.59	0.41
523	95% CO, 5% H_2	0.70	0.12	0.64	0.36
523	90% CO, 10% H_2	0.79	0.15	0.65	0.35
523	80% CO, 20% H_2	0.76	0.16	0.63	0.37
573	100% CO	0.74	0.08	0.58	0.42
573	90% CO, 10% H_2	0.61	0.31	0.57	0.43

[a] Monolayer fraction of adsorbed CO.
[b] Monolayer fraction of adsorbed C.
[c] Fraction of adsorbed CO which desorbs as CO during TPSR.
[d] Fraction of adsorbed CO which desorbs to CH_4 during TPSR.

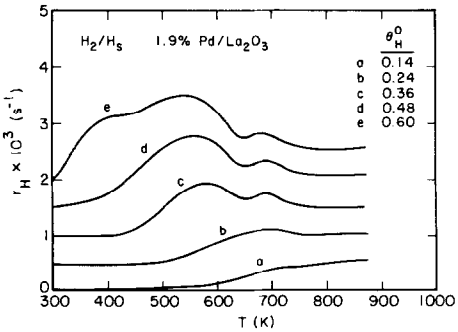

FIG. 7. Effect of initial coverage on the H_2 TPD spectra for 1.9% Pd/La_2O_3.

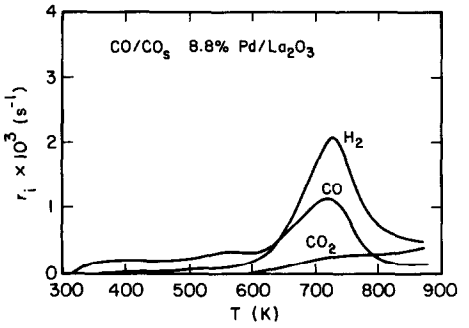

FIG. 8. Desorption products observed during TPD of CO adsorbed at 250 → 25°C on 8.8% Pd/La_2O_3.

La_2O_3 catalyst. The saturation coverage on the 8.8% Pd/La_2O_3 is 0.81, and a high-temperature tail is present.

At room temperature, no uptake of CO was observed on 8.8% Pd/La_2O_3. However, at elevated temperatures, a significant uptake was observed. Infrared studies reported by Hicks *et al.* (*18*) have shown that this uptake is due to the formation of formate structures. Figure 8 shows the features observed for desorption into He after the catalyst has been heated to 523 K, cooled to 298 K in flowing CO, and then evacuated at room temperature. A small amount of CO is seen to desorb at low temperatures, but a large peak appears at 723 K. A significant amount of H_2 is seen to desorb in a peak with the same location. In addition, a CO_2 tail is observed starting at 623 K. Thus, it appears that the formate structures decompose at around 723 K and undergo an interaction with the support which liberates H_2.

In contrast to the 8.8% Pd/La_2O_3 catalyst, infrared and chemisorption studies revealed that 1.9% Pd/La_2O_3 chemisorbs 0.34 of a monolayer of CO on the metal at room temperature (*18*). Figure 9 shows TPD spectra for CO adsorbed on the 1.9% Pd/La_2O_3 catalyst, taken at three different He flow rates. Notice that increasing the flow rate results in a larger degree of CO desorption. This is due to the lower concentrations of CO in the gas phase at high flow rates, which reduces the rate at which CO will react with the support to produce formates. For a carrier flow rate of 250 cm^3/min, a major peak is observed at 358 K along with a shoulder at 463 K. The peak at 723 K due to formate decomposition is still present. Even with this high flow rate, only 47% of the CO adsorbed is seen to desorb.

The sequential coadsorption of H_2 and CO was studied on the Pd/La_2O_3 catalysts. It was found that CO will not displace H_2 adsorbed on 8.8% Pd/La_2O_3. This is not surprising since CO will not chemisorb on a clean 8.8% Pd/La_2O_3 catalyst. On 1.9% Pd/La_2O_3, H_2 will not chemisorb on a sample

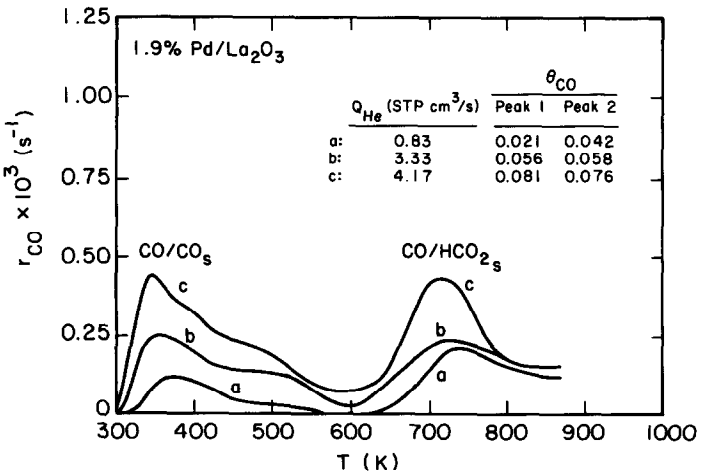

FIG. 9. Effect of flow rate on CO desorption during CO TPD from 1.9% Pd/La_2O_3.

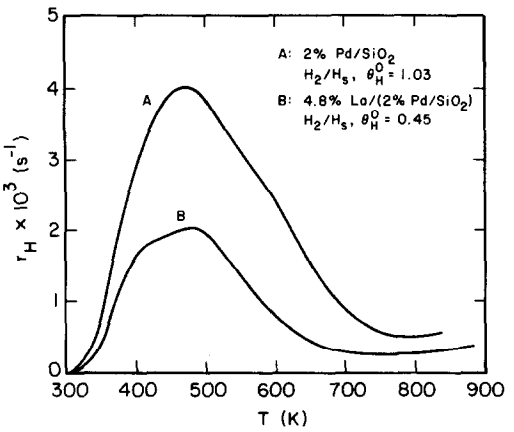

FIG. 10. Effect of lanthana promotion on H_2 desorption from Pd/SiO_2.

that has been saturated with CO. However, it was also observed that when the surface is first saturated with H_2 and then exposed to CO, the CO displaces only part of the H_2, leaving 0.29 of a monolayer on the surface. The resulting TPD spectrum is difficult to interpret due to the interaction of the CO with the support.

The TPD spectrum observed for H_2 desorption from lanthana-promoted Pd/SiO_2 is shown in Fig. 10. For comparison, an H_2 spectrum is also shown for desorption from unpromoted Pd/SiO_2. While the Pd dispersion of both catalysts, determined by H_2–O_2 titration, is the same, the maximum coverage at saturation on the lanthana-promoted Pd/SiO_2 is 0.45. The general shape and position of the spectra of the promoted and unpromoted samples are the same, suggesting that the nature of H_2 adsorption on both samples is similar. Consistent with this, it was observed that CO displaces adsorbed H_2 from lanthana-promoted Pd/SiO_2.

A comparison of the TPD spectra for CO desorption from promoted and unpromoted Pd/SiO_2 is given in Fig. 11. The spectrum for CO desorption from the promoted catalyst (B_1) is similar to that for the unpromoted catalyst (A_1), for temperatures below 380 K. At higher temperatures, spectrum B_1 shows a more rapid drop off than spectrum A_1, indicating that the strongly bound forms of CO are not as prevalent on the promoted as the unpromoted catalyst. The total amount of CO adsorbed initially on the two catalysts is also different: $\theta^0_{CO} = 0.45$ for the promoted catalyst and $\theta^0_{CO} = 0.88$ for the unpromoted catalyst. Three peaks are discernable in spectrum B_1. These occur at 383, 456, and 713 K. The positions of the

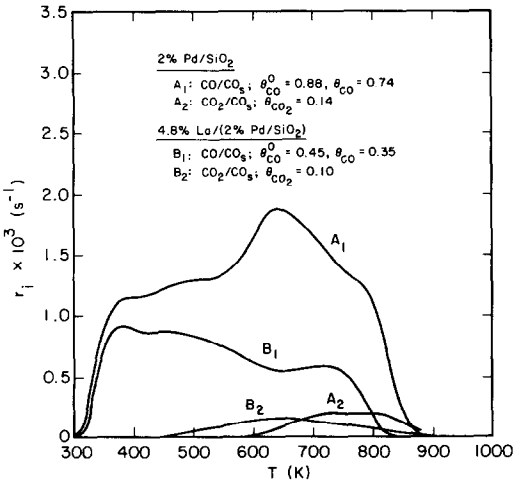

FIG. 11. Effect of lanthana promotion on the desorption products observed during CO TPD from Pd/SiO_2.

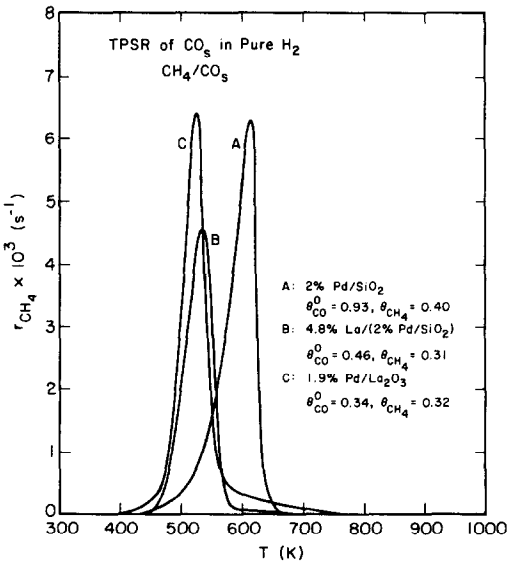

FIG. 12. Comparison of the TPSR spectra for CO adsorbed at 25°C on Pd/SiO_2, Pd/La_2O_3, and lanthana-promoted Pd/SiO_2.

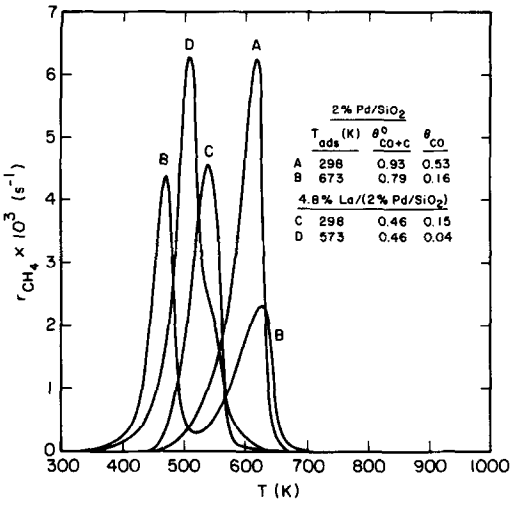

FIG. 13. Effects of CO adsorption temperature on the formation of CH_4 during TPSR of CO adsorbed on Pd/SiO_2 and lanthana-promoted Pd/SiO_2.

first two peaks are similar to those present in spectrum A_1, but the position of the third peak is 60 K lower than that of the corresponding peak in spectrum A_1.

The formation of CO_2 was observed to occur over lanthana-promoted Pd/SiO_2. As seen in Fig. 11, the onset of the CO_2 peak is 433 K. This is 165 K lower than the onset of CO_2 formation over unpromoted Pd/SiO_2. The fraction of the initially adsorbed CO which dissociates is 11% for the promoted sample and 8% for the unpromoted sample. Thus, lanthana promotion lowers the temperature at which CO disproportionation begins and increases the extent of CO disproportionation.

Figure 12 presents CH_4 spectra observed during the H_2 TPSR of CO adsorbed at room temperature on 1.9% Pd/La_2O_3, 2% Pd/SiO_2, and 4.8% La/(2% Pd/SiO_2). The feature for 2% Pd/SiO_2 is very similar to that seen for 9% Pd/SiO_2 in Fig. 4, and exhibits a maximum at 613 K. The amount of methane formed corresponds to 43% of the CO adsorbed initially. The spectrum for the lanthana-promoted Pd/SiO_2 shows a drastic decrease in the peak temperature to 536 K, which is near the peak for the 1.9% Pd/La_2O_3 at 525 K. For the lanthana-promoted catalyst, the amount of methane formed increases to 67% of the amount of CO adsorbed, while on the 1.9% Pd/La_2O_3, 94% of the CO reacts to give methane.

The effects of CO adsorption temperature on the TPSR spectra for promoted and unpromoted 2% Pd/SiO_2 are shown in Fig. 13. While experiments were also carried out with 1.9% Pd/La_2O_3, little useful information was obtained since the CH_4 features were broad and extended to high temperatures. Spectra A and B for unpromoted 2% Pd/SiO_2 are similar to the spectra seen in Fig. 5a for 9% Pd/SiO_2. Increasing the adsorption temperature to 673 K results in the appearance of a peak at 473 K due to to the hydrogenation of surface carbon and a reduction in the intensity of the peak near 610 K due to the hydrogenation of adsorbed CO. For lanthana-promoted Pd/SiO_2, raising the adsorption temperature to 573 K results in the formation of an intense peak at 510 K (spectrum D) and a reduction of the intensity of the peak at 536 K. Thus, promotion with lanthana results in an increase in the reactivity of adsorbed CO and an increase in the extent of CO disproportionation to surface carbon upon adsorption. A further effect of lanthana is a reduc-

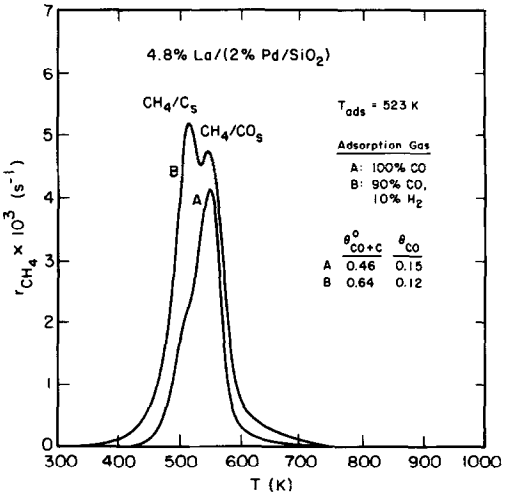

FIG. 14. Effects of the presence of H_2 during CO adsorption on the TPSR spectra for CH_4 formed over lanthana-promoted Pd/SiO_2.

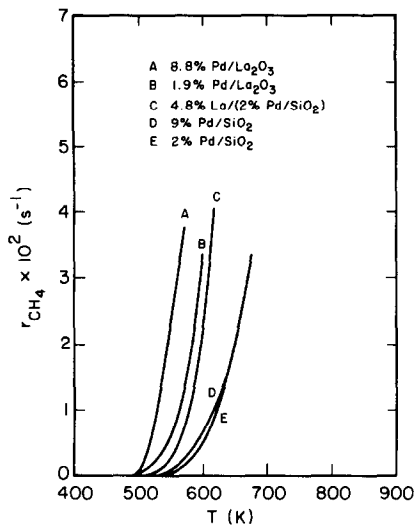

FIG. 15. Comparison of the methanation activities for Pd/SiO_2, Pd/La_2O_3, and lanthana-promoted Pd/SiO_2: p = 1 atm, H_2/CO = 3/1.

tion in the reactivity of adsorbed carbon. Figure 13 shows that the CH_4 peak for surface carbon hydrogenation occurs at a temperature 37 K higher for promoted Pd/SiO_2 than for unpromoted Pd/SiO_2.

Figure 14 shows the CH_4 spectrum for TPSR following adsorption at 523 K of pure CO and of 10% H_2 in CO. For pure CO, the peak at 536 K for CO methanation is essentially the same as that observed for room-temperature adsorption of CO. The small shoulder on the low-temperature side of the peak indicates that hydrogenation of surface carbon occurs to a limited degree. When CO is coadsorbed with H_2, the peak at 510 K becomes dominant, while the peak at 536 K increases slightly. Thus, as was the case for Pd/SiO_2, the presence of H_2 results in a buildup of surface carbon.

Comparison of Activities for CO Methanation

The influence of temperature on the rate of methane production over the five catalysts studied is shown in Fig. 15. In all cases, the maximum CO conversion does not exceed 1%. The activities follow the trend 8.8% Pd/La_2O_3 > 1.9% Pd/La_2O_3 > 4.8% La/(2% Pd/SiO_2) > 9% Pd/SiO_2 = 2% Pd/SiO_2. Promoting Pd/SiO_2 with lanthana results in an activity much closer to that of the La_2O_3-supported catalysts than the SiO_2-supported catalysts. The activation energies for methane formation were as follows: 8.8% Pd/La_2O_3, 43.1 kcal/mol; 1.9% Pd/La_2O_3, 40.3 kcal/mol; 4.8% La/(2% Pd/SiO_2), 33.5 kcal/mol; 9% Pd/SiO_2, 27.3 kcal/mol; 2% Pd/SiO_2, 27.5 kcal/mol.

No products of carbon number greater than one were observed on any of the catalysts. For the Pd/SiO_2 catalysts, water was the only product besides methane. However, the lanthana-promoted and La_2O_3-supported catalysts produced small amounts of methanol as shown in Fig. 16. For all three catalysts, the rate of methanol production passes through a maximum and then declines. The maximum rate of methanol formation for 8.8% Pd/La_2O_3 occurs at 538 K, while that for 1.9% Pd/La_2O_3 occurs at 563 K, and at 558 K for 4.8% La/(2% Pd/SiO_2). The lanthana-containing catalysts also displayed a significant water-gas shift activity. The turnover frequency for CO_2 production reached 1.0×10^{-2} s^{-1} at 563 K for 8.8% Pd/La_2O_3, 580 K for 1.9% Pd/

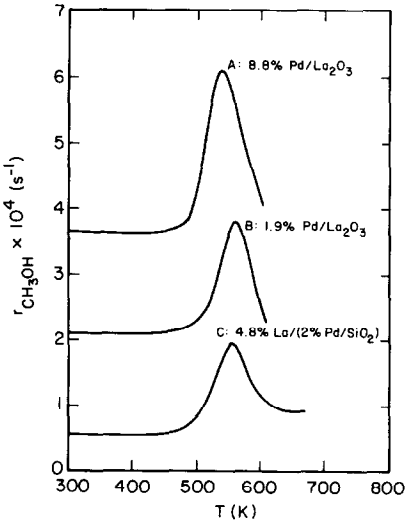

FIG. 16. Comparison of the activities for methanol synthesis for Pd/La_2O_3 and lanthana-promoted Pd/SiO_2: p = 1 atm, H_2/CO = 3/1.

La_2O_3, and 668 K for 4.8% La/(2% Pd/SiO_2).

DISCUSSION

Hicks *et al.* (*15–18*) have proposed that the surface of Pd particles supported on La_2O_3 is partially covered by oxygen-deficient lanthana moieties. This picture was deduced from XPS and CO chemisorption data. The XPS spectra of reduced Pd/La_2O_3 catalysts showed a systematic decline in the Pd $3d_{5/2}$ binding energy below the value for bulk Pd metal as the loading of Pd increased. Coincident with this was a decrease in the amount of CO chemisorbed per surface Pd atom. Hicks *et al.* (*17, 18*) argued that the LaO_x species on the surface of Pd physically block the adsorption of CO and act as a source of charge for shifting the binding energy of Pd immediately below, or in the vicinity of, the LaO_x moieties.

The TPR studies presented here support the contention of Hicks *et al.* (*17, 18*) that lanthana moieties in contact with Pd undergo a partial reduction. As was shown in Fig. 1, Pd particles are readily reduced at temperatures below 350 K. The peaks observed at 433 and 440 K in spectra A and B, for 8.8 and 1.9% Pd/La_2O_3, are ascribed to the partial reduction of lanthana in the vicinity of Pd, since these features are not observed for Pd/SiO_2 or La_2O_3 without Pd. While it is not possible to determine the fraction of reduced lanthana residing on the surface of Pd particles, it is evident that the amount of oxygen removed as H_2O from 8.8% Pd/La_2O_3 is greater than from 1.9% Pd/La_2O_3. Since the work of Hicks *et al.* (*17, 18*) indicates that Pd particles on the higher weight loading catalyst are more extensively covered than on the low weight loading catalyst, we conclude that the extent of lanthana reduction is enhanced by intimate contact between the metal and the overlying patches of lanthana.

The presence of lanthana as a support or promoter also appears to influence the reactivity of oxygen on Pd to reduction. This is evidenced by the removal of a part of the adsorbed oxygen at room temperature from Pd/La_2O_3 and lanthana-promoted Pd/SiO_2, but not from Pd/SiO_2, and by the lower peak temperature for Pd reduction observed for lanthana-containing catalysts.

The TPO experiments reveal that, under low partial pressures of O_2, Pd/SiO_2 consumes only enough O_2 to react off adsorbed H atoms. The uptake of O_2 by 4.8% La/(2% Pd/SiO_2) at room temperature exceeds this amount and the O_2 uptake on the Pd/La_2O_3 catalysts is even greater. The extra uptake of O_2 is ascribed to a reoxidation of the reduced portions of the support.

Pd/SiO₂

Two peaks are observed in the TPD spectra for H_2 desorption from the Pd/SiO_2 samples, both of which shift to lower temperature with increasing initial coverage, in accordance with second-order desorption kinetics. These features can be ascribed to H_2 desorption from different crystal surfaces of the supported Pd particles. The activation energy for H_2 desorption is 20.8 kcal/mol for a Pd(111) surface (*23*) and 24.5 kcal/mol for a Pd(100) surface (*24*). For both surfaces the activation energy remains nearly constant up to coverages close to saturation. Taking these values of the activation energies together with a preexponential factor of 10^{-2} cm^2/s for second-order desorption, we have calculated the peak positions anticipated for equilibrium desorption (*22*). The predicted peak positions for initially saturated surfaces are 560 K for the Pd(100) planes and 485 K for the Pd(111) planes. These values indicate that two peaks should indeed be discernable for desorption from a surface composed of a mixture of these planes. Since the area of the low-temperature peak is smaller than that of the high-temperature peak for both Pd/SiO_2 samples, we conclude further that the surface of the supported Pd particles consists predominantly of Pd(100) planes. This conclusion is in good agreement with the observations of Hicks *et al.* (*18*), who deduced the distribution of Pd planes from infrared spectra of adsorbed CO.

Three peaks are observed in the CO TPD spectrum for 9% Pd/SiO_2 and four are seen in the spectrum for 2% Pd/SiO_2. These features can be assigned on the basis of infrared observations reported by Hicks *et al.* (*18*). In that study, bands were observed at 2090, 1975, and 1920 cm^{-1}. These were assigned to CO linearly bonded on Pd(100) and Pd(111) planes, CO bridge-bonded on Pd(100) planes, and CO bridge-bonded on Pd(111) planes, respectively. Evacuation at 423 K for 1 h completely removed the band at 2090 cm^{-1}. Further evacuation at 573 K for 1 h resulted in a decrease in the intensity of the bands at 1975 and 1920 cm^{-1} until both were of the same magnitude. It is, therefore, evident that linearly bonded CO is more weakly adsorbed than bridge-bonded CO, and that bridge-bonded CO on Pd(100) planes is more weakly held than bridge-bonded CO on Pd(111) planes. Based on these observations, we attribute the peaks at 400 and 488 K, in the TPD spectra shown in Fig. 3, to linearly bonded CO adsorbed on Pd(100) and Pd(111) planes, respectively. Correspondingly, the two peaks at 638 and 773 K are attributed to CO bridge-bonded on Pd(100) and Pd(111) planes, respectively. As in the case of H_2 desorption, the peak associated with the Pd(100) planes is larger than that for the Pd(111) planes, indicating that Pd(100) predominate on the Pd particles.

The assignments given here for the two TPD peaks associated with bridge-bonded CO are also in agreement with the results of single-crystal studies (*25–27*). At zero coverage, the activation energy for CO desorption is 36 kcal/mol for Pd(100) planes and 34 kcal/mol for Pd(111) planes. As the CO coverage increases, the activation energies for both surfaces decrease in such a fashion that at high coverages the activation energy for Pd(100) surfaces is lower than that for Pd(111) surfaces. Hence, at high CO coverages, CO would be expected to desorb more readily from Pd(100) than Pd(111) surfaces. The shift of the TPD peak attributed to bridge-bonded CO adsorption on Pd(100) surfaces to higher temperatures with decreasing CO coverage is consistent with the reported increase in the activation energy for desorption from this plane.

As shown in Fig. 4, a small amount of CO_2 is produced above 600 K during the desorption of CO from 9% Pd/SiO_2. This is indicative of CO disproportionation. Similar results have been reported earlier by Rabo *et al.* (*28*), Doering *et al.* (*29, 30*), and Ichikawa *et al.* (*31*) for Pd supported on SiO_2 and mica, respectively. In the present study, it was also observed that the extent of CO disproportionation was the same for 2 and 9% Pd/SiO_2 samples, even though the dispersions of these catalysts differ by a factor of 2 (see Table 1). The average Pd particle sizes for these catalysts are 30 and 60 Å, respectively. It is interesting to note that Doering *et al.* (*29, 30*) also saw no effect of dispersion on the extent of disproportionation for particles in this size range. However, both Doering *et al.* (*29, 30*) and Ichikawa *et al.* (*31*) have reported that CO disproportionation occurs more readily on Pd particles that are less than 15 Å in size.

The results in Fig. 5a indicate that the extent of CO disproportionation increases significantly as the adsorption temperature increases above 573 K. This is evidenced by the growth in the CH_4 peak at 480 K attributed to hydrogenation of adsorbed carbon. The absence of a shift in the position of this peak suggests that the reactivity of the carbon is unaltered for CO adsorption temperatures as high as 673 K. This is surprising since the transformation of nascent carbon to less reactive forms occurs at much lower temperatures for metals such as Ni and Ru, which dissociate CO at lower temperatures than Pd (*28*). It should be noted though that the carbon deposited on Pd is much less reactive with respect to H_2 than carbon deposited on Ni and Ru, which reacts quantitatively at room temperature (*28, 32*). Nevertheless, the significantly higher reactivity of carbon on Pd with respect to adsorbed CO clearly indicates that the dissociation of CO to form carbon is the process limiting the methanation of adsorbed CO.

The dramatic increase in the amount of carbon deposited for high-temperature CO adsorption in the presence of small amounts of H_2 suggests that adsorbed H_2 may assist the dissociation of CO. An alternative explanation is that adsorbed H_2 reacts off O atoms to free more sites for CO dissociation. This latter possibility can be discounted for the following reasons. Oxygen adsorbed on a clean surface at temperatures from 298 to 573 K reacts off completely in pure H_2 at temperatures below 323 K. Thus, if the dissociation of CO resulted in a buildup of O atoms on the surface, a large water signal would be expected when H_2 was flowed over the catalyst at room temperature or in the early stages of the temperature ramp. No such feature was observed. In addition, when O_2 was adsorbed at temperatures from 298 to 573 K, complete removal was achieved by heating to 413 K in 408 ppm CO in He. During the adsorption step, 1 atm of CO is present, and the removal of O atoms should be facilitated by the higher CO pressure. Thus, there should be no buildup of O atoms inhibiting CO dissociation. Therefore, the logical explanation for the increase in the amount of surface carbon formed in the presence of H_2 is that H_2 participates in the dissociation step.

Several previous authors have suggested that H_2 assists or participates in the dissociation of CO on Pd and other Group VIII metals. This idea has been proposed by Mori *et al.* (*33*) to explain the more rapid methanation of adsorbed CO with D_2 than with H_2 over Pd/Al_2O_3. Wang *et al.* (*5*) have proposed a similar mechanism to explain their observations of CO hydrogenation over Pd supported on Al_2O_3, SiO_2, and TiO_2. Ho *et al.* (*34*) used a H_2-assisted dissociation step to explain the high activity of Ni for methanation, since the rate of carbon deposition from CO alone is much slower than the rate of methanation.

Pd/La_2O_3 and La_2O_3-Promoted Pd/SiO_2

The H_2 TPD spectra for 1.9% Pd/La_2O_3 and 4.8% La/(2% Pd/SiO_2) are qualitatively similar to those for the Pd/SiO_2 samples. As shown in Figs. 7 and 10, two H_2 peaks are observed. The principal difference is that the maximum amount of H_2 chemisorbed on the La_2O_3-containing catalysts corresponds to substantially less than a monolayer. The reduction in H_2 chemisorption may be attributable to the partial blockage of the Pd crystallites by patches of LaO_x.

It should be noted that the suppression of H_2 chemisorption on the 1.9% Pd/La_2O_3 sample reported here appears to contradict the results reported recently by Hicks *et al.* (*18*). Using standard volumetric adsorption techniques these authors measured a maximum H_2 uptake equivalent to one Pd monolayer. The discrepancy between the two measurements may well be due to the time allowed for H_2 to equilibrate with the sample. In the experiments reported here, H_2 was contacted with the catalyst for only a few minutes, whereas in the volumetric adsorption measurements, 1 to 2 h were allowed for equilibration at each H_2 pressure. Hicks *et al.* (*18*) proposed that the observation of an uptake of nearly one monolayer indicated that H_2 was adsorbed not only on the exposed Pd surfaces, but also on the LaO_x patches covering surface Pd atoms. If adsorption onto the latter type of site is slow, this would explain why only that portion of H_2 associated with Pd is observed in the TPD spectra shown in Figs. 7 and 10.

Comparison of the H_2 TPD spectra for Pd/SiO_2, Pd/La_2O_3, and La_2O_3-promoted Pd/SiO_2 indicates that the presence of La_2O_3 affects not only the quantity of H_2 adsorbed on Pd but also the strength of adsorption. For both La_2O_3-containing catalysts the lowest temperature peak occurs at 400 K, whereas for Pd/SiO_2 this peak occurs at 450 K. The position of the peak near 525–530 K appears to be independent of catalyst composition. Finally, in Fig. 10, one can observe a peak at 700 K, not seen in the spectrum for Pd/SiO_2. The origin of this peak is not fully understood. Three possibilities exist: H_2 adsorption on Pd; H_2

adsorption on LaO_x species covering Pd particles; and H_2 adsorption on La_2O_3 not in contact with Pd.

The interaction of CO with La_2O_3-supported Pd is complex because the CO adsorbs not only on the Pd particles, but also on the support itself. Infrared studies have shown that CO will react with hydroxyl groups on the support surface to form carbonate and formate structures (*18*) after the metal is saturated. This process is activated, and hence occurs more readily at higher temperatures. During a TPD experiment, CO desorbs from Pd particles at temperatures between 300 and 600 K. A fraction of the desorbing CO reacts to form formate and carbonate structures. Above 600 K, the formate structures decompose to liberate CO and a surface hydroxyl group or react with an additional hydroxyl group to produce H_2 and a carbonate group. These are the processes responsible for the high-temperature peaks observed in Figs. 8 and 9. Lanthanum carbonate is quite stable and decomposes only slowly at temperatures above 800 K. It is this process which is responsible for the slowly rising CO_2 signal seen in Fig. 8.

In spite of the complications just mentioned, it is apparent from Fig. 9 that supporting Pd on La_2O_3 results in a suppression of CO adsorption in the bridge-bonding states which give rise to TPD peaks at temperatures above 500 K. A similar effect is observed clearly in Fig. 11 for the La_2O_3-promoted Pd/SiO_2 catalyst. Since the formation of formate and carbonate structures was not observed for this sample, the total amount of CO adsorbed initially could be determined by integrating the TPD spectrum. As indicated in Fig. 11, the saturation level coverage by CO corresponds to 0.45 of a Pd monolayer. This figure is in good agreement with the saturation coverage by H_2 on the same catalyst (see Fig. 10).

The TPD spectra presented in Fig. 11 demonstrate that the promotion of Pd/SiO_2 with La_2O_3 results in a change in the distribution of adsorbed CO structures, in addition to a reduction in the overall capacity for CO adsorption. It is apparent from a comparison of spectra A_1 and B_1 that La_2O_3 promotion causes a preferential suppression of bridge-bonded CO relative to linearly bonded CO, and there is some indication that the binding strength of the high-temperature forms of CO is somewhat reduced.

The promotion of SiO_2-supported Pd with La_2O_3 greatly facilitates the dissociation of adsorbed CO to form carbon. This is clearly evident in Fig. 11, where the onset for CO disproportionation is seen to shift downscale by 125 K upon promotion. The data presented in Fig. 13 show that CO dissociation occurs much more readily over lanthana-promoted Pd/SiO_2 than over unpromoted Pd/SiO_2. The enhanced facility of CO dissociation is also responsible for the lowering of the peak temperature for methanation of adsorbed CO upon promotion (see Figs. 12 and 13).

Two mechanisms can be advanced to explain the effects of lanthana promotion on CO dissociation. The first is that the partially reduced LaO_x moieties present on the surface of the Pd particles transfer charge to the Pd thereby increasing the extent of back donation from the filled Pd *d*-orbitals to the unfilled $2\pi^*$ antibonding orbital of CO. This would have the effect of weakening the C–O bond. The second mechanism involves nucleophilic attack of the oxygen end of adsorbed CO by the reduced LaO_x species. In this case, dissociation of CO is facilitated through the action of LaO_x as an oxygen acceptor. This interpretation is similar to that recently proposed to explain the role of TiO_x (*12*) and MO_x (*35*, *36*) species in promoting CO methanation over Group VIII metals.

It is significant to note that as in the case of unpromoted Pd/SiO_2, the presence of H_2 enhances the degree of CO dissociation. This is clearly evident in Fig. 14. Possible explanations for the role of H_2 were discussed earlier in connection with Pd/SiO_2.

As seen in Fig. 13, the carbon produced

by CO dissociation in the presence of La_2O_3 is less reactive than that produced over unpromoted Pd/SiO_2. This effect of La_2O_3 is similar to that observed upon promotion with alkali metal oxides (*37–42*). Preliminary work in this laboratory with Na_2O-promoted Pd/SiO_2 has revealed that the carbon produced from CO dissociation is less reactive towards hydrogen than carbon formed on an unpromoted catalyst. A possible explanation for these effects is that promotion by lanthana and Na_2O strengthens the bond between carbon and Pd.

The higher specific activity for methanation of lanthana-supported Pd relative to silica-supported Pd reported here is in good agreement with the results of Hicks and Bell (*16*). Also consistent is the observation that the activation energy for Pd/La_2O_3 is considerably higher than that for Pd/SiO_2—41.7 versus 27.4 kcal/mol. Since promotion of Pd/SiO_2 with lanthana raises the activation energy to 33.5 kcal/mol, it is concluded that the higher activation energy observed with lanthana-containing catalysts is due to the decoration of the Pd crystallites by LaO_x moieties. These species must also be responsible for creating a very large number of active sites for methanation, which are needed to compensate for the higher activation energy. Thus, while the energetics of methane synthesis over Pd/La_2O_3 and lanthana-promoted Pd/SiO_2 are less favorable than over Pd/SiO_2, the much greater number of active sites on the former two catalysts contributed to their higher overall activities.

Hicks and Bell (*16*) have also demonstrated that the activation energy and reactant partial pressure dependences for methanol synthesis are virtually identical for Pd/SiO_2 and Pd/La_2O_3. Since the activity for Pd/La_2O_3 is greater than that for Pd/SiO_2, the implication is that the number of active sites on Pd/La_2O_3 is higher or alternatively that the surface populations of adsorbed H_2 and CO are altered to favor methanol synthesis. If we assume, as did Hicks and Bell (*16*), that the synthesis of methanol occurs on Pd metal rather than some type of special site, then it follows that the higher activity of Pd/La_2O_3 must be ascribed to a change in the coverages by H_2 and CO under reaction conditions. Since the present studies have shown that CO adsorption in strongly bound states is greatly suppressed when CO is supported on La_2O_3, we conclude that H_2 is more readily adsorbed on Pd/La_2O_3 than on Pd/SiO_2 under reaction conditions. This conclusion is supported by the observation that while CO will completely displace adsorbed H_2 from Pd/SiO_2, it will not from Pd/La_2O_3. Inasmuch as the catalytic properties of lanthana-promoted Pd/SiO_2 are similar to those of Pd/La_2O_3, the high methanol synthesis activity of lanthana-containing catalysts is attributed to the decoration of Pd crystallites by LaO_x moieties.

CONCLUSION

The present studies demonstrate that lanthana-promoted Pd/SiO_2 behaves quite similarly to Pd/La_2O_3, and exhibits properties quite different from those of unpromoted Pd/SiO_2. The unique properties of the lanthana-containing catalysts are attributed to the decoration of the supported Pd particles by partially reduced LaO_x moieties. These species suppress the chemisorption of H_2 and CO. While the distribution of H adstates is not altered significantly by LaO_x, the distribution of CO adstates is altered so as to greatly decrease adsorption into strongly bound states. The LaO_x species facilitate the dissociation of adsorbed CO to produce adsorbed carbon. This latter species is hydrogenated to CH_4 much more readily than adsorbed CO, indicating that the methanation over Pd proceeds via CO dissociation. A further finding of this study is that adsorbed hydrogen facilitates the dissociation of CO. The formation of methanol at 1 atm over Pd/La_2O_3 and lanthana-promoted Pd/SiO_2, but not Pd/SiO_2, is ascribed to an en-

hancement in the surface concentration of H relative to CO caused by the presence of LaO_x species on the Pd particles of the lanthana-containing catalysts.

ACKNOWLEDGMENT

This work was supported by the Division of Chemical Sciences, Office of Basic Energy Sciences, U.S. Department of Energy under Contract DE-AC03-76SF0098.

REFERENCES

1. Ichikawa, M., *Shokubai* **21,** 253 (1979).
2. Ryndin, Yu. A., Hicks, R. F., Bell, A. T., and Yermakov, Yu, I., *J. Catal.* **70,** 287 (1981).
3. Fajula, F., Anthony, R. G., and Lunsford, J. H., *J. Catal.* **73,** 237 (1982).
4. Vannice, M. A., *J. Catal.* **40,** 129 (1975).
5. Wang, S.-Y., Moon, S. H., and Vannice, M. A., *J. Catal.* **71,** 167 (1981).
6. Poels, E. K., van Broekhoven, E. H., van Barneveld, W. A. A., and Ponec, V., *React. Kinet. Catal. Lett.* **18,** 223 (1981).
7. Ponec, V., *Stud. Surf. Sci. Catal.* **11,** 63 (1982).
8. Poels, E. K., Koolstra, R., Geus, J. W., and Ponec, V., *Stud. Surf. Sci. Catal.* **11,** 233 (1982).
9. Driessen, J. M., Poels, E. K., Hindermann, J. P., and Ponec, V., *J. Catal.* **82,** 26 (1982).
10. Kikuzono, Y., Kagami, S., Naito, S., Onishi, T., and Tamaru, K., *Faraday Discuss. Chem. Soc.* **72,** 135 (1982).
11. Vannice, M. A., and Garten, R. L., *Ind. Eng. Chem. Prod. Res. Dev.* **18,** 186 (1979).
12. Bracey, J. D., and Burch, R., *J. Catal.* **86,** 384 (1984).
13. Yoshioka, H., Naito, S., and Tamaru, K., *Chem. Lett.*, 981 (1983).
14. Mitchell, M. D., and Vannice, M. A., *Ind. Eng. Chem. Fundam.* **23,** 88 (1984).
15. Hicks, R. F., and Bell, A. T., *J. Catal.* **90,** 205 (1984).
16. Hicks, R. F., and Bell, A. T., *J. Catal.* **91,** 105 (1985).
17. Fleisch, T. H., Hicks, R. F., and Bell, A. T., *J. Catal.* **87,** 398 (1984).
18. Hicks, R. F., Yen, Q.-J., and Bell, A. T., *J. Catal.* **89,** 498 (1984).
19. Low, G., and Bell, A. T., *J. Catal.* **57,** 397 (1979).
20. Uchida, M., and Bell, A. T., *J. Catal.* **60,** 204 (1979).
21. Chin, A. A., and Bell, A. T., *J. Phys. Chem.* **87,** 3700 (1983).
22. Rieck, J. S., and Bell, A. T., *J. Catal.* **85,** 143 (1984).
23. Conrad, H., Ertl, G., and Latta, E. E., *Surf. Sci.* **41,** 435 (1974).
24. Behm, R. J., Christmann, K., and Ertl, G., *Surf. Sci.* **99,** 320 (1980).
25. Conrad, H., Ertl, G., Koch, J., and Latta, E. E., *Surf. Sci.* **43,** 462 (1974).
26. Behm, R. J., Christmann, K., Ertl, G., and Van Hove, M. A., *J. Chem. Phys.* **73,** 2984 (1980).
27. Tracey, J. C., and Palmberg, P. W., *J. Chem. Phys.* **51,** 4852 (1969).
28. Rabo, J. A., Risch, A. P., and Poutsma, M. L., *J. Catal.* **53,** 295 (1978).
29. Doering, D. L., Poppa, H., and Dickinson, J. T., *J. Catal.* **73,** 104 (1982).
30. Doering, D. L., Poppa, H., and Dickinson, J. T., *J. Vac. Sci. Technol.* **17,** 198 (1980).
31. Ichikawa, S., Poppa, H., and Boudart, M., *J. Catal.* **91,** 1 (1985).
32. Wise, H., and McCarty, J. G., *Surf. Sci.* **133,** 311 (1983).
33. Mori, T., Masuda, H., Imai, H., Miyamoto, A., Hasebe, R., and Murakami, Y., *J. Phys. Chem.* **87,** 3648 (1983).
34. Ho, S. V., and Harriott, P., *J. Catal.* **64,** 272 (1980).
35. Sachtler, W. M. H., *in* "Proceedings, 8th International Congress on Catalysis," Vol. 1, p. 151. Verlag Chemie, Weinheim, 1985.
36. Sachtler, W. M. H., Shriver, D. F., Hollenberg, W. B., and Lang, A. F., *J. Catal.* **92,** 429 (1985).
37. Arakawa, H., and Bell, A. T., *Ind. Eng. Chem. Process Des. Dev.* **22,** 97 (1983).
38. Bonzel, H. P., and Krebs, H. J., *Surf. Sci.* **109,** L527 (1981).
39. Gonzalez, R. D., and Mirua, H., *J. Catal.* **77,** 338 (1982).
40. McClory, M. M., and Gonzalez, R. D., *J. Catal.* **89,** 392 (1984).
41. Goodman, D. W., and Kiskinova, M., *Surf. Sci.* **105,** L265 (1981).
42. McVicker, G. B., and Vannice, M. A., *J. Catal.* **63,** 25 (1980).